
Uncertainty Intervals for Graph-based Spatio-Temporal Traffic Prediction

Tijs Maas
Informatics Institute,
University of Amsterdam
tijs_maas@hotmail.com

Peter Bloem
INDELab,
University of Amsterdam
uva@peterbloem.nl

Abstract

Many traffic prediction applications rely on uncertainty estimates instead of the mean prediction. Statistical traffic prediction literature has a complete subfield devoted to uncertainty modelling, but recent deep learning traffic prediction models either lack this feature or make specific assumptions that restrict its practicality. We propose Quantile Graph Wavenet, a Spatio-Temporal neural network that is trained to estimate a density given the measurements of previous timesteps, conditioned on a quantile. Our method of density estimation is fully parameterised by our neural network and does not use a likelihood approximation internally. The quantile loss function is asymmetric and this makes it possible to model skewed densities. This approach produces uncertainty estimates without the need to sample during inference, such as in Monte Carlo Dropout, which makes our method also efficient.

1 Introduction

Currently, most traffic prediction models predict the average traffic conditions from minutes 5 up to an hour ahead. While impressive, this problem setting largely ignores the uncertainty of the generated predictions, making the results more difficult to interpret. Many real-world applications rely on confidence intervals or certainty bounds for these predictions, instead of the mean predicted value. For example, when scheduling road maintenance or when planning a route with minimal delays.

Using Monte Carlo (MC) Dropout [1], it is possible to model the trips within a city, and utilize vehicle trajectories to predict future traffic speeds [2, 3]. This technique requires B stochastic forward passes to compute the sample variance. Increasing the number of stochastic inference samples B improves the quality variance. Monte Carlo (MC) Dropout makes the assumption that uncertainty in traffic speed and volume can be modelled as multivariate Gaussian. The reality however, is that these distributions are skewed and asymmetric and thus do not satisfy the assumption made here. For instance, when the traffic speed is measured to be maximum, it is far more likely to decrease than increase.

In this extended abstract, we introduce a novel traffic prediction model based on the spatio-temporal neural network Graph Wavenet [4]. However, instead of optimizing our mean prediction, we train using a Quantile loss function, similar to Autoregressive Implicit Quantile Networks [5]. This makes it possible to estimate the density at specific points, conditioned on a quantile. Our method allows for non-gaussian uncertainty modelling, which remains greatly unexplored in the deep learning traffic prediction literature. The contribution of this work can be summarized as follows:

- We introduce a method to approximate asymmetric and skewed density functions to model the uncertainty estimate.
- Instead of approximating the variance using multiple forward passes, our technique requires only one pass for each requested density quantile.

2 Quantile Regression

Quantile Regression is a method to estimate the quantile function of a distribution at chosen points, which is equal to the inverse cumulative distribution function (cdf). It has been shown that when minimized using stochastic approximation, quantile regression converges to the true quantile function value [6]. This allows us to approximate a distribution using a neural network approximation of its quantile function, acting as reparameterization of a random sample from the uniform distribution.

Let us define the quantile regression loss $\rho_\tau(u) = (\tau - \mathbb{I}[u \leq 0])u$ [6] for the error u and the quantile $\tau \in \mathcal{U}[0, 1]$. When u is positive F underestimates Z i.e. the estimate falls short of the true value. Now for a given scalar distribution Z with cdf F_Z and a quantile τ we obtain the inverse cdf $F_Z^{-1}(\tau) = q$, which minimizes the expected quantile regression loss $\mathbb{E}_{z \sim Z}[\rho_\tau(z - q)]$.

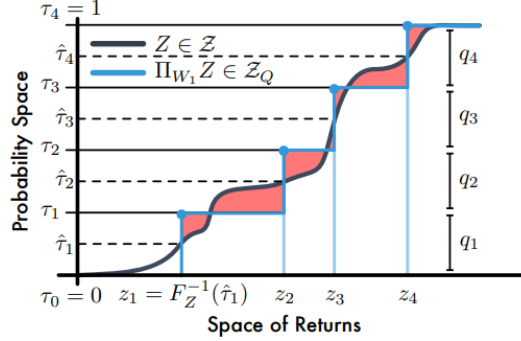


Figure 1: 1-Wasserstein minimizing projection Π_{W_1} onto $N = 4$ uniformly weighted Diracs. Shaded regions sum to form the 1-Wasserstein error. For detailed explanation, we refer the reader to [7].

3 Graph WaveNet

Graph WaveNet is neural network architecture for spatio-temporal traffic prediction. Different from the AIRAI competition, this model assumes traffic measurements in the form of sensors on a road network graph. The architecture consists of temporal causal convolutions (TCN) [8] with graph diffusion convolutions applied to every layer.

3.1 Temporal Convolutions

Gating mechanisms are critical in recurrent neural networks and they have been shown to be powerful to control information flow through layers for temporal convolution networks as well. The gating mechanism in Graph Wavenet is two parallel TCN layers configured with a gate:

$$\mathbf{h} = g(\Theta_1 \star \mathcal{X} + \mathbf{b}) \odot \sigma(\Theta_2 \star \mathcal{X} + \mathbf{c}) \quad (1)$$

Specifically, the LSTM-style gating ($g = \tanh$) also shared with PixelCNN [9] and WaveNet [10] is used.

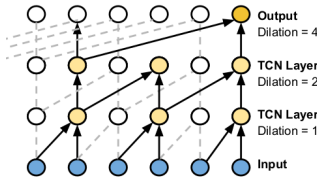


Figure 2: Dilated casual convolution with kernel size 2 and dilation factor k , it picks inputs every k step and applies the standard 1D convolution to the selected inputs.

Another advantage is that the temporal receptive field grows exponentially w.r.t. the number of layers and the dilation factor. To achieve this, we artificially design the receptive field size of Graph

WaveNet equals to the sequence length of the inputs so that in the last spatial-temporal layer the temporal dimension of the outputs exactly equals to one. After that we set the number of output channels of the last layer as a factor of step length T to get our desired output dimension.

3.2 Spatial Graph Diffusion Convolution

Graph Wavenet uses spatial graph convolution [11] to share information on the graph structure. This type of graph convolution differs from the popularised GCN of Kipf and Welling [12], since it is based on epidemic diffusion [13]:

$$\mathbf{X}_{:,c} \star_{\mathcal{G}} f_{\theta} = \sum_{k=0}^{K-1} \left(\theta_{k,1} (\mathbf{D}_O^{-1} \mathbf{W})^k + \theta_{k,2} (\mathbf{D}_I^{-1} \mathbf{W}^{\top})^k \right) \mathbf{X}_{:,c} \quad \text{for } c \in \{1, \dots, C\} \quad (2)$$

where $\theta \in \mathbb{R}^{N \times 2}$ are the filter parameters and $\mathbf{D}_O^{-1} \mathbf{W}, \mathbf{D}_I^{-1} \mathbf{W}^{\top}$ represent the transition matrices of the diffusion process and the reverse one, respectively. They note that since $T_{k+1} = (\mathbf{D}_O^{-1} \mathbf{W}) T_k(x)$ and $\mathbf{D}_O^{-1} \mathbf{W}$ is sparse, it is possible to use recursive sparse-dense matrix multiplication arriving at a time complexity $O(K|\mathcal{E}|)$ of their update function, which is similar in complexity to the method proposed by Kipf and Welling. However, unlike the method of Kipf and Welling, the edges between the nodes are non-symmetric. Another advantage is that this method only uses a sparse graph neighbourhood in its update function, rather than the full graph Laplacian, and is therefore more resilient against structural changes.

3.3 Loss Function

The training objective is the Mean Absolute Error (MAE) over Q prediction timesteps, N locations, each with C different measurements.

$$L(\hat{\mathbf{X}}^{(t+1):(t+Q)}; \Theta) = \frac{1}{QNC} \sum_{i=1}^Q \sum_{j=1}^N \sum_{k=1}^C \left| \hat{\mathbf{X}}_{jk}^{(t+i)} - \mathbf{X}_{jk}^{(t+i)} \right| \quad (3)$$

4 Quantile Graph WaveNet

We modify Graph WaveNet to implicitly predict the cdf, instead of optimizing for the mean prediction error. This involves conditioning the input on a quantile τ and training with a quantile loss function.

One drawback to the original quantile regression loss is that gradients do not scale with the magnitude of the error, but instead with the sign of the error and the quantile weight τ [5]. The Huber quantile regression loss introduces a threshold κ , such that if the error is within the threshold κ , scaling is performed w.r.t. the magnitude of the errors. In our experiments we find that $\kappa = 0.05$ works well.

$$\rho_{\tau}^{\kappa}(u) = |\tau - \mathbb{I}\{u \leq 0\}| \mathcal{L}_{\tau}^{\kappa}(u), \quad \text{with } \mathcal{L}_{\tau}^{\kappa}(u) = \begin{cases} \frac{1}{2\kappa} u^2 & \text{if } |u| < \kappa \\ |u| - \frac{1}{2}\kappa & \text{otherwise} \end{cases}$$

5 Data Preparation

We evaluate our model on traffic in Los Angeles (METR-LA [14]), Istanbul and Berlin[15]. The dataset METR-LA recorded 207 loop detectors in the metropolitan area of Los Angeles from March 1st, 2012 until June 30th, 2012. We partition this timeline into 3 non-overlapped sections: training, validation and test with the respective ratios 7:1:2.

The Traffic4cast competition offers more complicated real-world datasets from the cities: Berlin, Istanbul and Moscow. The data is presented as grid with the resolution of 495x436 pixels for each city, and every pixel constitutes 100m². The training and validation set contain 181 and 18 days, respectively. In their main challenge it is expected from participants to make 500 predictions of up to 1h into the future (test set), spread over 163 days.

The Berlin and Istanbul dataset are an excellent opportunity to test our uncertainty prediction model on a larger scale. However, Graph WaveNet expects a sensors on a graph, which is different from the 495x436x9 image in the competition. In theory, one could consider every pixel as a node on the

\mathcal{D}	Measurement locations	Duration	No measurement
METR-LA	207	34272	0.08
ISTANBUL	999	52128	0.61
BERLIN	1336	52128	0.77

Table 1: Traffic dataset statistics (after preprocessing).

graph, however it is the case that most pixels report traffic measurements infrequently. In contrast to METR-LA, where the percentage of operational sensors is typically $> 90\%$, as seen in Table 1. For practicality reasons, we sampled pixels from the $495 \times 436 \times 9$ image with a value density of at least $\frac{1}{16}$ in the outskirts and $\frac{1}{2}$ towards the city centre. From the remaining pixels we sample equidistant points ($d = 1200\text{m}$) on the traffic graph, in Berlin this yields a graph of approximately 1300 nodes. Measurements of the average traffic speed are used at an interval of 5 minutes.

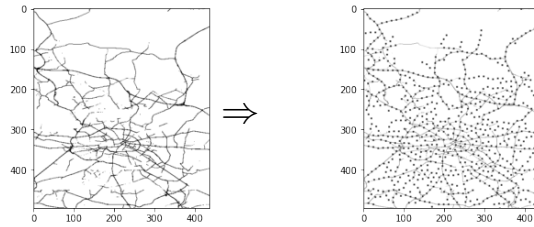


Figure 3: Extraction of equidistant measurement locations on the traffic network.

6 Results

We evaluate the results of our model on the datasets METR-LA, ISTANBUL and BERLIN. Since we do not have the complete test set of ISTANBUL and BERLIN, we instead have partitioned the 181 days training set into train, validation and test with the ratio: (0.89, 0.01, 0.10). Our main results are the uncertainty estimates and their calibration, we compare this to MC Dropout uncertainty estimates. Additionally, we also provide the mean prediction accuracy and compare this with previous methods.

Qualitative results To demonstrate that we can successfully learn uncertainty intervals that are skewed and asymmetric, we plot the 0.9 CI in Figure 4, for both Graph WaveNet with the proposed Quantile estimation and Graph WaveNet with MC Dropout. We also project the mean prediction of the original measurements. The locations of the sensors are visible in the map on the left.

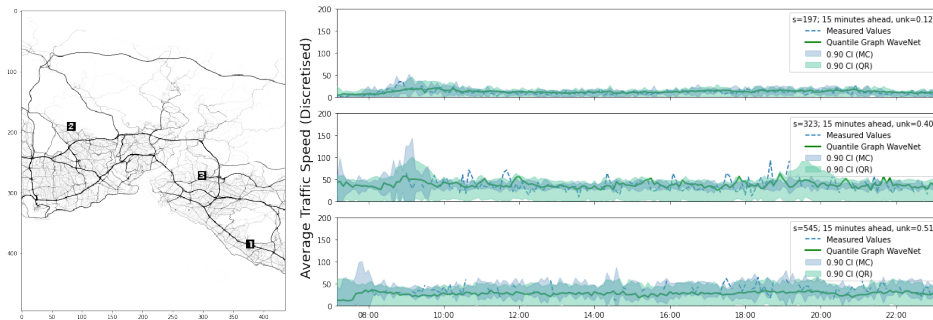


Figure 4: Randomly selected sensors grouped by percentage of given measurements.

A benefit of the Quantile uncertainty interval (lightgreen) is that each boundary or mean is generated by a distinct τ value, on which the network is conditioned. This is efficient to compute and greatly improves the flexibility of uncertainty intervals, which is expressed as skewed and asymmetric densities.

Calibrated uncertainty After training, we need to calibrate our model on the validation set. Figure 5 shows the uncertainty calibration of BERLIN: before calibration, after calibration on the validation set and on the test set.

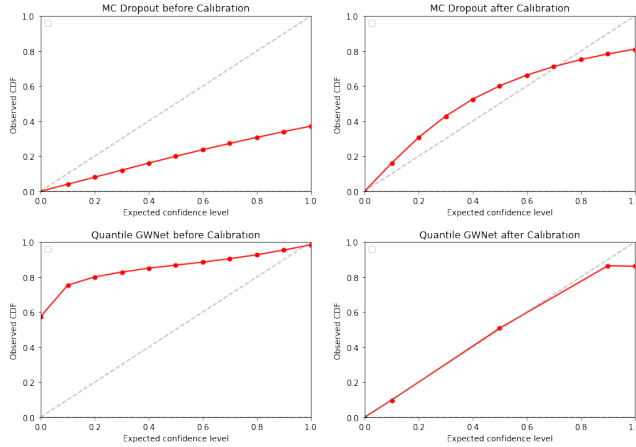


Figure 5: Expected confidence vs observed cdf, before and after calibration on the validation set.

Both Monte Carlo Dropout and Quantile Graph WaveNet require an additional calibration step, however the advantage of the latter is that we can re-map every tau value, as suggested by [16]. The underestimation that is present in many Bayesian Neural networks [16] is not present in the Quantile Graph WaveNet. However, recalibration by reassigning the Quantiles is not perfect either since exploring the region outside of what is learned may cause the density to decrease rather than increase as wished. We do assume the CDF to start with 0.0 and end with 1.0, but there is no mathematical law that requires this start- and endpoint. In theory we can shrink and expand our space if needed, but retraining on these areas with remapped tau values may help prevent reversal of the density.

Mean prediction accuracy Lastly, we compare the mean prediction accuracies for the default Graph Wavenet and our proposed Quantile Graph Wavenet (denoted by Quantile est in table below). Note that this is just to demonstrate the difference and this is not the main contribution of this research.

\mathcal{D}	Model	15 min		30 min		60 min	
		MAE	MSE	MAE	MSE	MAE	MSE
METR-LA	Hist. Average	5.18	81.18	5.18	81.18	5.18	81.18
	Static Pred.	4.03	75.86	5.11	124.32	6.82	202.77
	Graph WaveNet [†]	2.69	26.62	3.08	38.81	3.50	53.14
	↔ Dropout MC [†]	2.71	27.14	3.13	39.81	3.60	55.50
	↔ Quantile est. [†]	3.90	38.68	3.95	42.25	4.05	45.56
ISTANBUL	Hist. Average*	23.63	852.64	23.63	852.64	23.63	852.64
	Static Pred.	11.06	313.99	11.22	320.05	11.53	331.96
	Graph WaveNet [‡]	5.58	131.79	5.66	136.30	5.80	144.00
	↔ Dropout MC [‡]	5.80	129.53	5.89	134.00	6.09	141.14
	↔ Quantile est. [‡]	6.16	168.66	6.32	176.82	6.61	192.22
BERLIN	Hist. Average*	19.18	520.29	19.18	520.29	19.18	520.29
	Static Pred.	12.48	778.96	12.59	791.85	12.77	807.69
	Graph WaveNet [‡]	7.38	234.09	7.45	244.60	7.61	252.81
	↔ Quantile est. [‡]	7.74	318.00	7.83	326.05	8.00	338.48
	↔ after calibr. [‡]	7.77	320.41	7.86	328.38	8.02	340.76

[†] : The mean of 3 experiments.

* : Historical weekly averages, predictions of missing values are counted as average target prediction

error.

‡ : Results of 1 experiment, the adaptive adjacency matrix is not enabled in the model.

We observe a decrease in the mean prediction accuracy if we compare Graph Wavenet with its Quantile estimation counterpart, and this is consistent for all datasets. A possible explanation why Quantile Graph WaveNet performs worse on the Traffic4cast datasets may be due to more frequently missing measurements. The versatility of Quantile Graph WaveNet can also be a weakness, using the same number of parameters to predict for any quantile, almost certainly reduces the complexity of the mean approximation. For instance if the density to be learned is shaped differently from the mean. Quantile Graph Wavenet predicts on a subset of the pixelspace used by the Traffic4cast competition and direct accuracy score comparison with other contestants should be avoided. However, making a fair comparison is possible by masking the pixels not used in the graph and computing the MSE of the active pixels. This table omits many recently proposed models and for a comprehensive study on traffic prediction models, we refer the reader to [17].

7 Discussion

The method presented here is a step towards reliable traffic prediction uncertainty estimates. Initial results appear promising but we also want to highlight the limitations of our method.

1. Crossing quantiles: define two quantiles τ_1 and τ_2 , with $\tau_1 < \tau_2$, then we should never have that $f(x, \tau_1) < f(x, \tau_2)$.
2. Uncertainty missing for missing values: estimating a density when there are no values has no solution.
3. Additional calibration step is required after training.

Since uncertainty intervals are highly useful in traffic prediction applications, we believe that densities beyond the Gaussian should be considered the topic of future research. We chose to model the density directly, following a technique developed in Reinforcement Learning, thereby omitting the likelihood computation all together. In conjunction, more descriptive confidence metrics such as [18] and [19] could be developed with traffic prediction uncertainty applications in mind.

Broader Impact

Improvements in traffic prediction have the potential to improve traffic conditions and reduce travel delays by facilitating better utilization of the available capacity. Traffic uncertainty estimation allows better planning for scheduled road maintenance and uncertainty estimates are more informative when routing critical trips.

Acknowledgments and Disclosure of Funding

Work done partly during internship at HAL24K.

References

- [1] Yarin Gal and Zoubin Ghahramani. Dropout as a Bayesian Approximation: Representing Model Uncertainty in Deep Learning. *arXiv:1506.02142 [cs, stat]*, October 2016.
- [2] Lingxue Zhu and Nikolay Laptev. Deep and Confident Prediction for Time Series at Uber. In *2017 IEEE International Conference on Data Mining Workshops (ICDMW)*, pages 103–110, November 2017.
- [3] Xitong Zhang, Liyang Xie, Zheng Wang, and Jiayu Zhou. Boosted Trajectory Calibration for Traffic State Estimation. In *2019 IEEE International Conference on Data Mining (ICDM)*, pages 866–875, Beijing, China, November 2019. IEEE.
- [4] Zonghan Wu, Shirui Pan, Guodong Long, Jing Jiang, and Chengqi Zhang. Graph WaveNet for Deep Spatial-Temporal Graph Modeling. *arXiv:1906.00121 [cs, stat]*, May 2019.

- [5] Georg Ostrovski, Will Dabney, and Rémi Munos. Autoregressive Quantile Networks for Generative Modeling. *arXiv:1806.05575 [cs, stat]*, June 2018.
- [6] Roger Koenker and Kevin F. Hallock. Quantile Regression. *Journal of Economic Perspectives*, 15(4):143–156, December 2001.
- [7] Will Dabney, Mark Rowland, Marc G. Bellemare, and Rémi Munos. Distributional Reinforcement Learning with Quantile Regression. *arXiv:1710.10044 [cs, stat]*, October 2017.
- [8] Yann N. Dauphin, Angela Fan, Michael Auli, and David Grangier. Language Modeling with Gated Convolutional Networks. *arXiv:1612.08083 [cs]*, September 2017.
- [9] Aaron van den Oord, Nal Kalchbrenner, Oriol Vinyals, Lasse Espeholt, Alex Graves, and Koray Kavukcuoglu. Conditional Image Generation with PixelCNN Decoders. *arXiv:1606.05328 [cs]*, June 2016.
- [10] Aaron van den Oord, Sander Dieleman, Heiga Zen, Karen Simonyan, Oriol Vinyals, Alex Graves, Nal Kalchbrenner, Andrew Senior, and Koray Kavukcuoglu. WaveNet: A Generative Model for Raw Audio. *arXiv:1609.03499 [cs]*, September 2016.
- [11] Yaguang Li, Rose Yu, Cyrus Shahabi, and Yan Liu. Diffusion Convolutional Recurrent Neural Network: Data-Driven Traffic Forecasting. *arXiv:1707.01926 [cs, stat]*, February 2018.
- [12] Thomas N. Kipf and Max Welling. Semi-Supervised Classification with Graph Convolutional Networks. *arXiv:1609.02907 [cs, stat]*, February 2017.
- [13] Kristina Lerman and Rumi Ghosh. Network structure, topology, and dynamics in generalized models of synchronization. *Physical Review E*, 86(2):026108, August 2012.
- [14] H. V. Jagadish, Johannes Gehrke, Alexandros Labrinidis, Yannis Papakonstantinou, Jignesh M. Patel, Raghu Ramakrishnan, and Cyrus Shahabi. Big Data and Its Technical Challenges. *Commun. ACM*, 57(7):86–94, July 2014.
- [15] David P. Kreil, Michael K. Kopp, David Jonietz, Moritz Neun, Aleksandra Gruca, Pedro Herruzo, Henry Martin, Ali Soleymani, and Sepp Hochreiter. The surprising efficiency of framing geo-spatial time series forecasting as a video prediction task – Insights from the IARAI Traffic4cast Competition at NeurIPS 2019. In *NeurIPS 2019 Competition and Demonstration Track*, pages 232–241. PMLR, August 2020.
- [16] Volodymyr Kuleshov, Nathan Fenner, and Stefano Ermon. Accurate Uncertainties for Deep Learning Using Calibrated Regression. *arXiv:1807.00263 [cs, stat]*, June 2018.
- [17] Xueyan Yin, Genze Wu, Jinze Wei, Yanming Shen, Heng Qi, and Baocai Yin. A Comprehensive Survey on Traffic Prediction. *arXiv:2004.08555 [cs, eess]*, April 2020.
- [18] Max-Heinrich Laves, Sontje Ihler, Karl-Philipp Kortmann, and Tobias Ortmaier. Well-calibrated Model Uncertainty with Temperature Scaling for Dropout Variational Inference. *arXiv:1909.13550 [cs, stat]*, November 2019.
- [19] Dan Levi, Liran Gispan, Niv Giladi, and Ethan Fetaya. Evaluating and Calibrating Uncertainty Prediction in Regression Tasks. *arXiv:1905.11659 [cs, stat]*, February 2020.